Progress in Reaction Kinetics and Mechanism

ARTICLE

Open Access

https://doi.org/10.48130/prkm-0026-0004

Progress in Reaction Kinetics and Mechanism **2026**, 51: e012

Study on the performance of chemical kinetic mechanism models for methanol/DME blended fuel

Hua Xiao[1#], Chenlong Xie[1,2#], Zhihao Ma[2*], Youcai Liang[3] and Xin Li[4]

[1] *School of Ocean Engineering, Guangzhou Maritime University, Guangzhou 510725, China*
[2] *School of Vehicle and Traffic Engineering, Henan University of Science and Technology, Luoyang 471003, China*
[3] *School of Electric Power, South China University of Technology, Guangzhou 510640, China*
[4] *School of Vehicle and Mobility, Tsinghua University, Beijing 100084, China*
[#] Authors contributed equally: Hua Xiao, Chenlong Xie
[*] Correspondence: mazhihao@haust.edu.cn (Ma Z)

Abstract

The co-combustion of methanol and dimethyl ether (DME) presents a promising approach for achieving efficient and low-emission combustion in engines. To comprehensively evaluate the applicability of detailed chemical kinetic mechanisms for methanol/DME blends, six existing mechanisms from the literature were systematically assessed using an integrated approach combining numerical simulation and experimental measurement. The analysis focused on various key parameters, including ignition delay times (IDT), laminar burning velocity (LBV), and concentrations of different critical intermediate species. For the first time, LBV data for methanol/DME blends at various mixing ratios were experimentally measured using the heat flux method in the present work, providing critical data for mechanism validation. In terms of IDT prediction, the Yan mechanism demonstrated the highest accuracy across different pressures, equivalence ratios, and blend ratios, while the Aramco 2.0 mechanism also performed well under most conditions. For LBV prediction, the Yan mechanism provided the most reliable predictions for methanol and DME under high-pressure conditions, whereas the Aramco 2.0 mechanism yielded the smallest overall prediction error for blended fuels under atmospheric pressure. Species concentration simulations revealed that both the Aramco 2.0 and Yan mechanisms captured the variation trends of CO, CO_2, and CH_2O with temperature reasonably well. However, discrepancies can be observed in CH_2O predictions around 800 K, indicating variations in the configuration of reaction pathways. Overall, the Yan and Aramco 2.0 mechanisms show high reliability in characterizing the combustion behavior of methanol/DME blended fuels. The choice between these mechanisms should be guided by the specific pressure conditions in practical applications.

Citation: Xiao H, Xie C, Ma Z, Liang Y, Li X. 2026. Study on the performance of chemical kinetic mechanism models for methanol/DME blended fuel. *Progress in Reaction Kinetics and Mechanism* 51: e012 https://doi.org/10.48130/prkm-0026-0004

Introduction

The swift consumption of conventional energy sources has led to a worsening greenhouse effect. Against this backdrop, methanol has emerged as a low-carbon and renewable energy carrier, gradually developing into a promising alternative fuel. As the simplest alcohol compound, methanol possesses significant potential as an alternative fuel and is often referred to as 'liquid sunshine'[1]. Methanol's liquid state at ambient temperature and pressure distinguishes it from gaseous alternatives like natural gas, ammonia, and hydrogen, enabling easy and cost-effective storage and transport using established petroleum infrastructure[2]. Feedstock flexibility allows methanol to be synthesized from coal, natural gas, or biomass, among others, demonstrating strong resource sustainability. It can also be synthesized by combining carbon dioxide with hydrogen generated from renewable energy sources[3,4]. In addition, as an oxygenated fuel, owing to the absence of C–C bonds, methanol minimizes soot formation and also lowers oxygen demand during combustion[5]. Methanol also has a high heat of vaporization, which can effectively reduce combustion temperatures; however, this characteristic also poses significant challenges, especially during cold-start conditions[6,7]. Furthermore, the low reactivity of methanol restricts its utilization in compression ignition engines. To achieve compression ignition, this challenge can be mitigated by employing high-cetane fuels or ignition improvers[8,9]. DME, the simplest ether compound, has a cetane number of 55–60, which is higher than that of diesel fuel[10]. The production of DME via methanol dehydration is feasible, and through waste heat utilization, the catalytic reaction can be sustained during engine operation[11].

Studies have shown that blending two fuels with significantly different ignition characteristics is an effective method to be used in compression ignition engines for combustion control[12,13]. DME and methanol have been the focus of considerable research as promising clean alternative fuels. According to fuel design theory, methanol, with its high octane number, can help mitigate knock under high-load conditions, while DME, with its high cetane number, can broaden the ignition range. The use of methanol/DME blended fuels in homogeneous charge compression ignition (HCCI) engines therefore allows for clean, high-efficiency combustion across a wide range of operating conditions. Through numerical simulations, Yao et al.[14] investigated the combustion and emission characteristics of methanol/DME blends in HCCI engines, validating their results against experimental data. The simulation results demonstrated close agreement with the experimental data. Lee et al.[15] computationally investigated the HCCI combustion of DME-methanol blends. Their results indicated that methanol addition elevates the peak heat release rate and pressure rise rate, thereby increasing the propensity for engine knock. Taghavifar et al.[16] studied the HCCI combustion characteristics of multicomponent diesel-DME/methanol blends. Their results demonstrated that a higher DME concentration extends the ignition delay and raises the heat release rate.

To more effectively utilize methanol/DME blended fuels, a thorough understanding of their reaction mechanisms is crucial. Practical combustion systems, such as engine combustion chambers, require more specific studies on the reaction processes of methanol/DME mixtures. Some progress has already been made in this area. Using an RCM, Wang et al.[17] measured the IDT of methanol/DME blends. Their investigation revealed that the unimolecular decomposition of HO_2CH_2OCHO has a significant influence on the low-temperature ignition process. Song et al.[18] used simulations to examine DME's effect on methanol blend ignition delay. They found that at 850 K, DME-derived low-temperature species play a critical role in facilitating auto-ignition. In addition, Yan et al.[19] investigated DME oxidation in an SP-JSR. Their results showed that at 100 atm, the NTC behavior is weaker than at 10 atm, and the intermediate temperature oxidation window shifts to lower temperatures. Burke et al.[20] measured IDTs for DME, methane, and DME/methane mixtures using a shock tube (ST) and a rapid compression machine (RCM), and constructed a new kinetic model. The study found that the incorporation of a Quantum-Rice-Ramsperger-Kassel (QRRK) treatment for pressure-dependent low-temperature oxidation reactions was essential for accurate predictions of DME's IDTs. Wang et al.[21] studied DME oxidation in a laminar flow reactor and developed a refined sub-mechanism via rate constant analysis and theoretical calculations. This improved mechanism accurately describes DME's oxidation behavior across low and intermediate temperature ranges. Hashemi et al.[22] investigated the pyrolysis and oxidation of DME and DME/methane mixtures in a laminar flow reactor. Their results showed that DME exhibits an NTC region which, while sensitive to equivalence ratio, consistently occurs between 575 and 625 K. Reuter et al.[23] studied DME combustion in a counterflow burner. Their results indicated that at a fixed fuel mass fraction, blending methane with DME raises the high-temperature extinction limit while lowering the low-temperature one.

The primary objective of this work is to evaluate different DME kinetic mechanisms and identify the model that most accurately captures the combustion behavior of methanol/DME blended fuels. In this study, six DME kinetic mechanisms published in the literature between 2014 and 2022 were selected to investigate their performance in simulating the combustion of methanol/DME blends. They are the Yan mechanism[19], the Aramco 2.0 mechanism[20], the Wang mechanism[21], the Hashemi mechanism[22], the Reuter mechanism[23], and the Pelucchi mechanism[24]. The Yan mechanism, which comprises 130 species and 894 elementary reactions, is an updated version based on the Reuter mechanism. It incorporates revisions to the reaction rates of relevant chemical reactions using research findings from Klippenstein[25,26], Zhao[27], and Mulvihill[28], among others. The updated mechanism improves upon the original by enabling accurate prediction of species concentrations after the oxidation of DME under high-pressure conditions. The Reuter mechanism was developed to address the low-temperature oxidation chemistry coupling of DME and CH_4 blended mixtures. It was constructed by systematically studying the extinction limits of hot flames, cool flames, and ozone-assisted cool flames using a counterflow burner experimental platform. The mechanism was updated based on the work of Zhao et al.[29], resulting in a final mechanism containing 130 species and 893 elementary reactions. The Wang mechanism, consisting of 78 species and 301 elementary reactions, was derived from the Zhao mechanism. It was refined by incorporating research results from Carr[30] and Sivaramakrishnan[31] to update key reaction pathways and rate constants. The Hashemi mechanism, which includes 102 species and 894 elementary reactions, was developed specifically for CH_4/DME blends. It was constructed on the basis of an H_2/C1/C2 alcohol sub-mechanism, integrating the formic acid sub-mechanism from Marshall and Glarborg[32], with each DME-related reaction being individually evaluated. The Aramco 2.0 mechanism was developed by the University of Galway and contains 176 species and 2,716 elementary reactions, including a DME sub-mechanism. The Pelucchi mechanism was developed by Politecnico di Milano and consists of 356 species and 10,171 elementary reactions, also incorporating a sub-mechanism for DME. Although not all of these mechanisms were originally developed specifically for methanol/DME combustion, it is meaningful to validate them and extend their applicability by comparing their performance, especially for engine relevant conditions, as shown in Table 1. To assess the performance of each kinetic mechanism, this study investigates IDT, LBV, and species concentrations for methanol/DME blended fuels.

Experimental and numerical methods

Experimental methods

To validate different kinetic models, experimental data from relevant literature was utilized, as summarized in Table 2. Due to the lack of LBV data for methanol/DME mixtures, preliminary measurements were conducted in this work using the heat flux method (HFM), as shown in Fig. 1. The heat flux was developed and refined by De Goey et al.[33], enabling flame stabilization on a perforated plate burner. The fundamental principles can be found in the work of Wang et al[34]. The core advantage of using a heat flux burner to measure LBV lies in its ability to create and stabilize an unstretched, one-dimensional flat flame, thereby avoiding the complex and error-prone extrapolation processes required by other methods. The platform mainly consists of the heat-flux burner, a fuel supply

Table 1. Basic information on the model referenced.

Model	Species	Reactions	Fuel system	Methods/objects	Conditions	Year	Ref.
Yan	130	894	DME	SP-JSR/species	T = 400–900 K, p = 10, 100 atm, φ = 0.175–1.72, t = 0.1–1 s	2022	[19]
Aramco 2.0	176	2,716	CH_4/DME	RCM/IDT; ST/IDT	T = 600–1,600 K, p = 7–41 bar, φ = 0.3–2.0, CH_4, DME, CH_4/DME = 80/20, 60/40	2014	[20]
Wang	78	301	DME	JSR/species; Laminar flow reactor/species	T = 400–1,160 K, p = 1–40 atm, φ = 0.6–1.2	2014	[21]
Hashemi	102	894	CH_4/DME	Laminar flow reactor/species; LBV	T = 450–900 K, p = 1–100 bar, φ = 0.06–20, t = 4–22 s, χ_{DME} = 1.8%–3.6%, 100%	2019	[22]
Pelucchi	356	10,171	toluene/n-heptane	Theory and modeling/rate constants and model validation; ST, RCM/IDT; JSR/species; Flame speed measurements/LFS	T = 300–2,500 K, p = 0.1–1,000 bar, φ = 0.2–5.0	2018	[24]
Reuter	130	893	CH_4/DME	Counterflow burner/flames	p = 0.1 MPa, φ = 0.25–1.5, χ_{DME} = 0%–100%	2018	[23]

Table 2. Experimental data used in the study.

Fuel/oxidizer	Methods	Specified initial conditions	Date used in the study	Year	Ref.
Methanol/DME/O_2/N_2	RCM	T = 585–910 K, p = 15–30 bar, φ = 0.5–2	IDT	2018	Wang et al.[17]
Methanol/DME/air	HFM	T = 298 K, p = 1 atm, φ = 0.7–1.4	LBV	2025	This study
Methanol/air	HFM	T = 298 K, p = 1 atm, φ = 0.7–1.4	LBV	2021	Wang et al.[34]
Methanol/air	CVCC	T = 298–425 K, p = 0.5–3.5 bar, φ = 0.8–1.6	LBV	2004	Saeed et al.[35]
Methanol/air	HFM	T = 298–358 K, p = 1 bar, φ = 0.7–1.5	LBV	2014	Sileghem et al.[36]
Methanol/air	HFM	T = 298–358 K, p = 1 bar, φ = 0.7–1.5	LBV	2012	Vancoillie et al.[37]
Methanol/air	CVCC	T = 298–700 K, p = 0.4–50 atm, φ = 0.8–1.5	LBV	1982	Metghalchi et al.[38]
DME/air	HFM	T = 298 K, p = 1 atm, φ = 0.7–1.7	LBV	2018	Wang et al.[39]
DME/air	CVCC	T = 298 K, p = 1–10 atm, φ = 0.7–1.6	LBV	2005	Qin et al.[40]
DME/air	CVCC	T = 303–493 K, p = 0.1 MPa, φ = 0.7–1.6	LBV	2015	Yu et al.[41]
DME/air	CVCC	T = 295 K, p = 1 bar, φ = 0.7–1.7	LBV	2001	Daly et al.[42]
DME/air	Counterflow burner	p = 0.1 MPa	LBV	2009	Wang et al.[43]
Methanol/O_2/N_2	JSR	T = 700–1,200 K, p = 10 atm, φ = 1, t = 0.05 s	Concentration of CH_2O, CO, CO_2	2016	Burke et al.[44]
DME/O_2/N_2	JSR	T = 500–900 K, p = 10 atm, φ = 0.175, t = 0.12–0.07 s	Concentration of CH_2O, CO, CO_2	2022	Yan et al.[19]

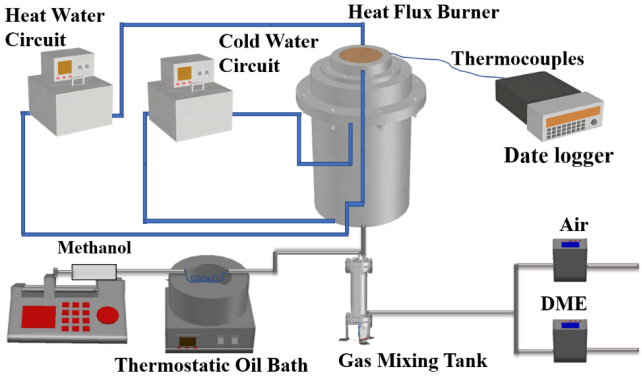

Fig. 1 Experimental setup for laminar burning velocity.

system, and a temperature monitoring system. The gases of air and DME used in the experiments were regulated by Azbil digital mass flow controllers. Methanol is delivered using a micro-syringe pump and then passes through an evaporation system to ensure complete vaporization before being introduced into the heat flux burner. This study measures the LBV of blended fuels with DME molar fractions of 40% and 80% under atmospheric pressure, a temperature of 298 K, and φ = 0.7–1.4.

The uncertainty in this study originates mainly from three sources: errors associated with the mass flow controllers, errors in temperature measurement within the heat flux burner, and fluctuations in the initial temperature.

Error introduced by the mass flow controller can be shown as:

$$\Delta S_{\mathrm{L}} = (\Delta F_{fuel} + \Delta F_{\mathrm{N2}} + \Delta F_{\mathrm{O_2}})/600\,A$$

where, ΔS_{L} represents the uncertainty of the mass flow controller, in cm/s, A is the surface area of the furnace pan of the heat flow meter, in m^2, and ΔF denotes the uncertainty of the flow rate of the mass flow controller, in L/min.

ΔF is calculated as follows:

$$\Delta F = 0.8\%R_{\mathrm{d}} + 0.2\%F_{\mathrm{S}}$$

where, R_{d} represents the reading of the mass flow meter, and Fs denotes its range. According to the manufacturer's recommendation, the mass flow meter should be operated above 10% of its minimum range for optimal accuracy.

There are errors in the temperature distribution measurement of the eight thermocouples on the furnace pan of the heat flow meter. The error due to temperature measurement can be shown as:

$$\sigma_{S_{\mathrm{L}}} = \frac{1}{s}\frac{2\sigma_{tc}}{r_{\mathrm{b}}^2}$$

where, s is the sensitivity parameter, corresponding to the derivative value of the temperature distribution curve when the parabolic factor β is 0, σ is the mean standard deviation of the thermocouples (0.8 K), and r_{b} is the radius at the outermost thermocouple i.e., 14.7 mm.

The error of the equivalence ratio can be calculated as follows:

$$\Delta\phi/\phi = \Delta F_{fuel}/F_{fuel} + \Delta F_{\mathrm{O_2}}/F_{\mathrm{O_2}}$$

Based on detailed uncertainty analysis calculations, the experimental accuracy for the LBV measurements stays within ± 1 cm/s.

Numerical methods

Ignition delay modeling

The IDT is defined as the period from the End of Compression to the time at which the first derivative of pressure with respect to time reaches its maximum value. In premixed combustion, this key property is largely dictated by the mixture's reactivity[45]. IDT is primarily influenced by fuel composition, temperature, and pressure. Predicting IDT through numerical simulations not only allows for a deeper understanding of the chemical kinetics involved in the combustion process, but also helps optimize the design and operation of combustion systems by employing simplified mechanisms and selecting appropriate kinetic parameters. In both research and engineering applications, calculating IDT is a key tool for achieving efficient and low-emission combustion. In practice, IDT is commonly measured using ST and RCM during experiments, as in previous studies[17,46]. Due to viscosity, heat transfer, and non-equilibrium effects during experiments, deviations from ideal conditions occur. Therefore, inert gases are often used to highly dilute the fuel/oxidizer mixture to minimize the influence of these factors on experimental measurements.

This study uses the Closed Homogeneous Batch Reactor in CHEMKIN-PRO software and performs RCM simulations by varying the reactor volume to account for the specific effects of the RCM. During the simulations, methanol/DME blended fuels were diluted with nitrogen to minimize the effects of viscosity, heat transfer, and non-equilibrium phenomena, as encountered in RCM experiments[47]. A series of numerical simulations covering extensive pressure, temperature, and equivalence ratio conditions were carried out to reproduce the experimental data from Wang et al.[17].

Laminar burning velocity modeling

LBV is a key parameter for characterizing premixed combustion flames and a fundamental metric for validating detailed chemical kinetic mechanisms. In this study, LBV was simulated using the PREMIX module, which models steady-state, one-dimensional, freely propagating flames. The simulations account for thermo-diffusion (Soret effect) and employ a multicomponent diffusion approach to describe molecular diffusion. In addition to the flame speed, the simulation provides temperature profiles, species concentration distributions, and reaction rate distributions. Furthermore, reaction sensitivity analyses—such as sensitivities of laminar flame speed or temperature—can be conducted during computation to support more in-depth reaction kinetics studies. The numerical conditions in this work correspond to the experimental setup reported by Wang et al.[34], enabling comparison of LBV predictions from different chemical mechanisms across a range of equivalence ratios.

Jet stirred reactor modeling

Jet stirred reactors (JSRs) are essential devices for studying the oxidation behavior of species at various temperatures. They are typically coupled with instruments such as gas chromatographs (GC), gas chromatography-mass spectrometry (GC-MS), and flue gas analyzers to enable real-time detection of the experimental fuel and its oxidation products under different operating conditions. In this study, simulations of JSR experiments were conducted using the transient solver in the Perfectly Stirred Reactor (PSR) module. This module allows for the calculation of the concentrations of reactants, intermediates, and final products during the reaction process. Sensitivity analysis and reaction pathway analysis can also be performed during the simulation, facilitating a more in-depth investigation of reaction kinetics. The numerical simulation conditions in this study are similar to those used in the experiments conducted by Burke et al. and Yan et al.[19,44], and are employed to compare species concentrations predicted by different mechanisms under various conditions.

Results and discussion

Ignition delay time analysis

Since Wang et al. have conducted comprehensive experiments on the IDTs of methanol/DME, the study begins its validation with IDT. To investigate the accuracy of existing methanol/DME mechanisms in predicting IDT, simulations were conducted for methanol/DME blended fuels with varying DME mole fractions (25%, 50%, and 75%), φ = 0.5, 1, 2, and p = 15, 30 bar. The simulation results were validated using the experimental data reported by Wang et al. For clarity, in this study, 'C' represents methanol, 'D' represents DME, and the numbers indicate the corresponding fuel proportion.

Figure 2a shows the variation of IDT with the inverse of temperature for a C50D50 mixture at an φ = 1, under p = 15 bar. As shown in Fig. 2a, the Yan mechanism demonstrates the best prediction performance. The predictions from the Pelucchi and Aramco 2.0 mechanisms are relatively close, but slower than those of the Yan mechanism when the temperature exceeds 750 K. The Hashemi mechanism predicts faster IDTs than the Yan mechanism overall. The Wang and Reuter mechanisms yield similar results, showing a trend of over-prediction (shorter IDT) at low temperatures and under-prediction (longer IDT) at high temperatures compared to the Yan mechanism. As illustrated in Fig. 2b, when the pressure increases from 15 bar to 30 bar, all mechanisms tend to underestimate the IDT at low temperatures, with the Yan mechanism exhibiting the smallest error. Reasonable predictions of the blended fuel's IDT are provided by the Pelucchi, Aramco 2.0, Wang, and Reuter mechanisms. The prediction accuracy of the Hashemi mechanism significantly improves with increasing pressure.

Figure 2a, c, and d show the IDT variation with temperature for the C50D50 mixture at 15 bar and φ = 0.5, 1.0, and 2.0, respectively. Figure 2c reveals a discrepancy between the Yan mechanism and experimental data, where the model's overprediction of IDTs increases with temperature. Other mechanisms also show certain deviations, but their predictions generally fall within the experimental uncertainty. As illustrated in Fig. 2d, the Yan and Aramco 2.0 mechanisms show the best agreement, with good consistency at temperatures below 750 K. At temperatures above 750 K, the Aramco 2.0 mechanism demonstrates better accuracy than the Yan mechanism. The Pelucchi mechanism exhibits a similar trend to the Aramco 2.0 mechanism but with larger errors. The Wang and Reuter mechanisms yield comparable results and show a tendency to overpredict IDT (shorter delay) at temperatures below 700 K. The Hashemi mechanism deviates significantly from the experimental data, consistently predicting much shorter IDTs. Overall, from Fig. 2a, c, and d, the Yan and Aramco 2.0 mechanisms provide the most accurate predictions of ignition delay under varying equivalence ratios.

At 15 bar and 800 K, with φ = 0.5, 1, and 2, a brute-force sensitivity analysis was conducted for the C50D50 mixture to explore the differences among various mechanisms. In this context, A negative value of the sensitivity coefficient signifies ignition promotion, while a positive value signifies inhibition. As shown in Fig. 3a and b, the most sensitive reactions during ignition calculations using the Yan and Aramco 2.0 mechanisms were compared. It is clear that the reactions $CH_3OCH_3 + OH = CH_3OCH_2 + H_2O$, and $CH_3OCH_3 + HO_2 = CH_3OCH_2 + H_2O_2$ are the most effective in promoting ignition in both mechanisms. However, the most inhibiting reactions differ significantly between the two mechanisms: for the Yan mechanism, $CH_2OCH_2O_2H = OH + 2CH_2O$ has the strongest inhibiting effect, while for the Aramco 2.0 mechanism, $CH_3OH + OH = CH_2OH + H_2O$ is the most inhibitory. In fact, differences in the rate constants of certain key reactions can greatly affect the prediction of ignition. For example, for the highly promoting reaction $CH_3OCH_3 + OH = CH_3OCH_2 + H_2O$, the rate constant is $k = 2.32 \times 10^5$ in the Yan mechanism and $k = 9.35 \times 10^5$ in the Aramco 2.0 mechanism. This case illustrates how such differences in rate parameters can significantly alter predictive performance in ignition simulations.

Figure 2a, e, and f respectively show the difference of IDT with temperature for blended fuels at different mixing ratios under conditions of 15 bar and a φ = 1.0. As shown in Fig. 2e, all mechanisms except for the Yan mechanism exhibit a trend of overpredicting IDT at low temperatures and under-predicting it at high temperatures. The Yan mechanism, however, shows accurate predictions at low temperatures, with increasing deviation as temperature rises. Nonetheless, the prediction errors of all mechanisms fall within the experimental uncertainty range. In Fig. 2f, the Aramco 2.0 mechanism demonstrates relatively accurate predictions, while the others show slight deviations from the experimental data. Considering Fig. 2a, e, and f together, the accuracy of the Yan mechanism is evident in its predictions of methanol/DME blend IDTs across various mixing ratios. Therefore, to illustrate the kinetic differences among blended fuels with varying mixing ratios, a sensitivity analysis was conducted using the Yan mechanism, as shown in Fig. 3c. The analysis was performed under conditions of 15 bar, 800 K, and an equivalence ratio of 1 for C25D75, C50D50, and C75D25 blended fuels. The results indicate that for the C50D50 and

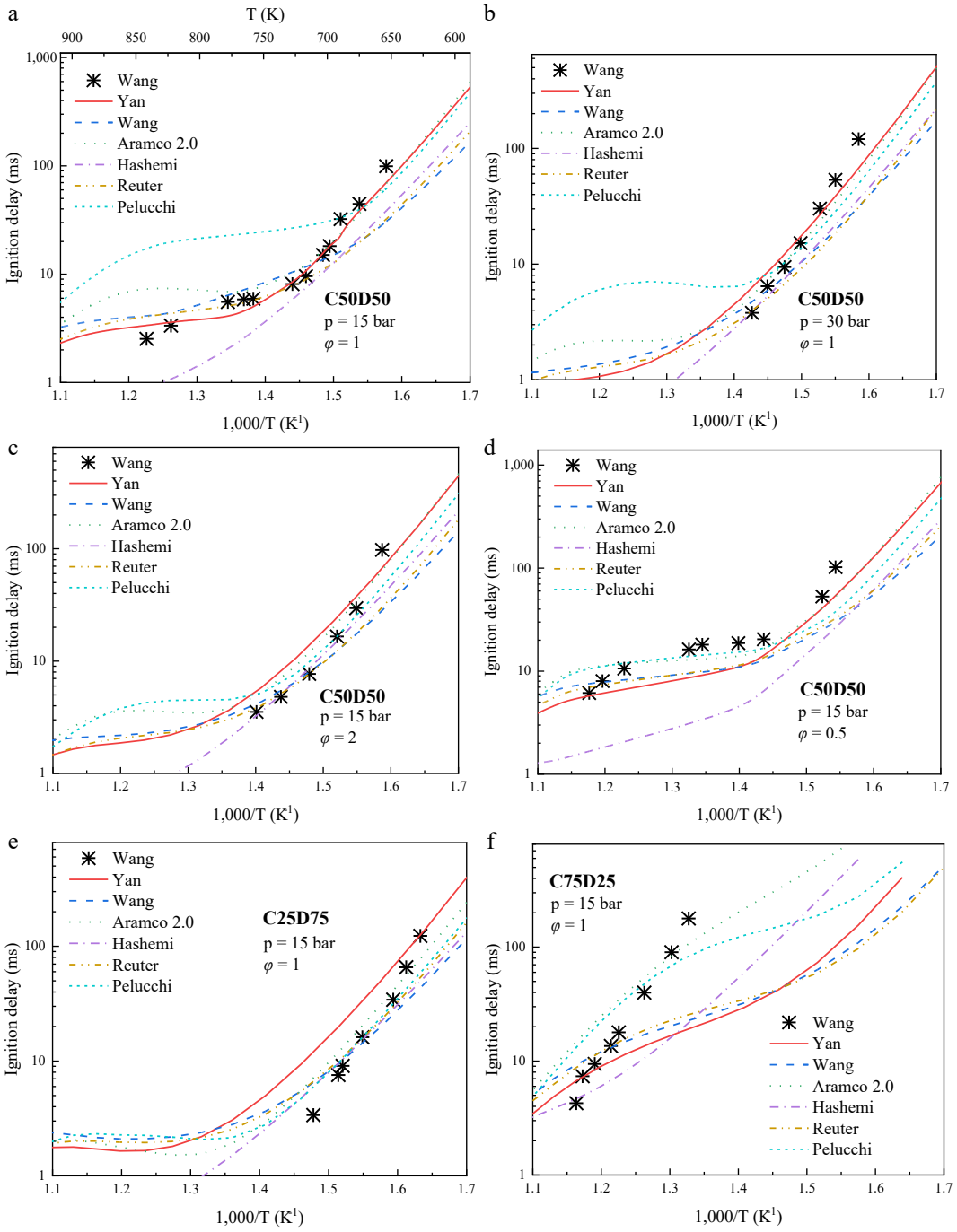

Fig. 2 Variation of IDT for methanol/DME blended fuels with 1000/T: RCM data (symbols) vs simulation results from various mechanisms (lines).

C75D25 blends, the reaction R795 ($CH_3OCH_3 + HO_2 = CH_3OCH_2 + H_2O_2$) has the most significant promoting effect on ignition, and the sensitivity coefficient S_{R795} exhibits a linear relationship with the methanol/DME ratio—the higher the methanol content, the greater the sensitivity of IDT to S_{R795}. For the C75D25 blend, reactions R824 and R48 are the two most influential promoting reactions. Regarding ignition inhibition, the most influential inhibiting reactions vary among the different blended fuels. Interestingly, reaction R187 promotes ignition for the C50D50 and C75D25 blends, but is the most inhibitive reaction for the C25D75 blend.

A comprehensive validation of six kinetic mechanisms using RCM data across various pressures, equivalence ratios, and blending ratios shows that the Yan mechanism emerges as the most reliable for IDT prediction. The Aramco 2.0 mechanism also provides highly satisfactory predictions. Additionally, the Wang and Reuter mechanisms demonstrate relatively high predictive accuracy in most cases.

Laminar burning velocity analysis

To further evaluate the performance of existing kinetic mechanisms in predicting the LBV of premixed methanol/DME flames, simulations were conducted for pure methanol, pure DME, C20D80, and C60D40 mixtures under various equivalence ratios. The simulation results were validated against experimental data for pure methanol and DME according to Wang et al.[25,26]. Figure 4 shows the simulated flame speeds of pure methanol, pure DME, C20D80,

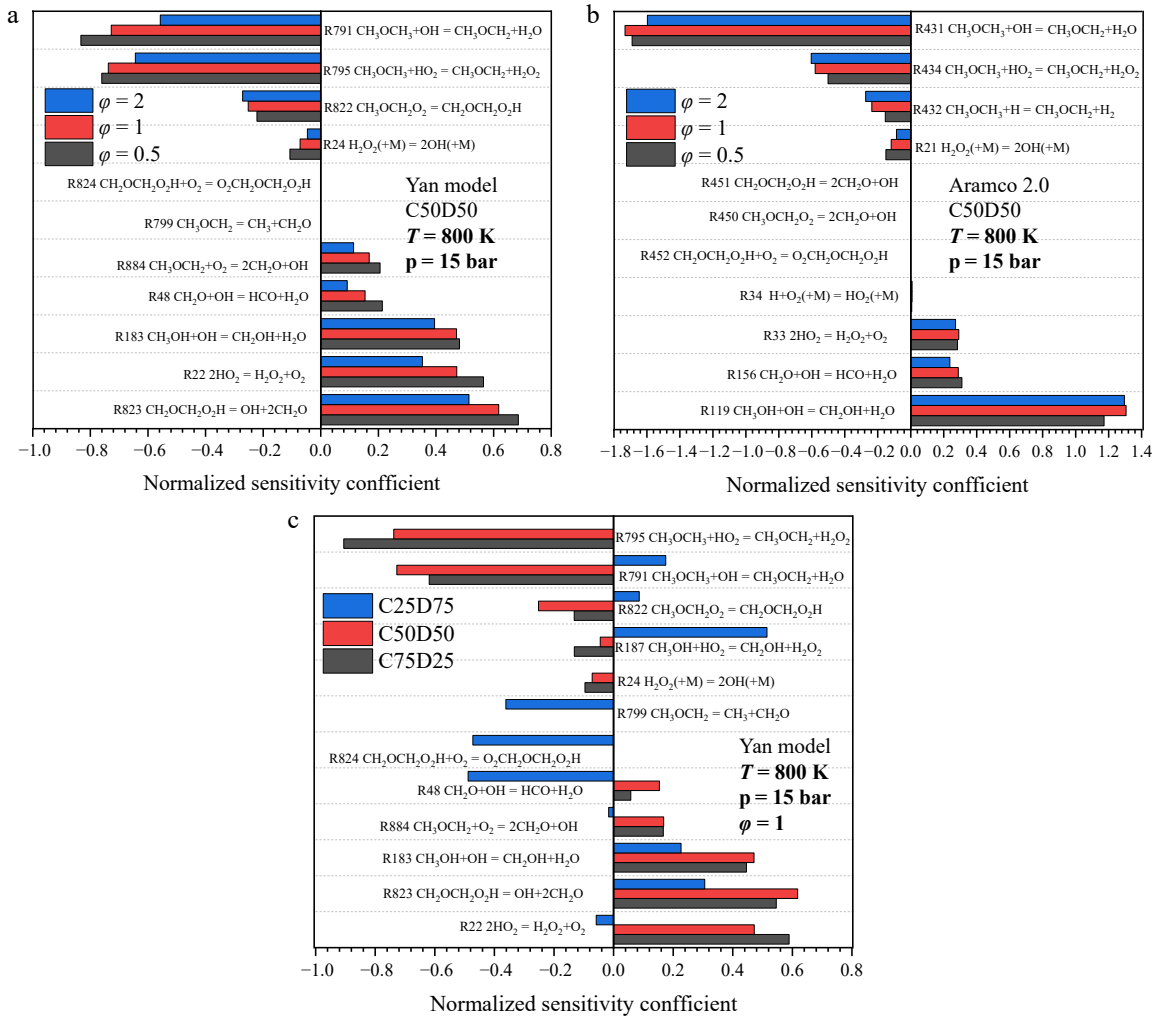

Fig. 3 Sensitivity analyses of the (a) Yan model, and (b) Wang model under different equivalence ratios. (c) Sensitivity analysis of the Yan model under different blending ratios.

and C60D40 using different DME mechanisms. The simulations reveal a non-monotonic dependence of LBV on the equivalence ratio, characterized by an initial increase followed by a decrease.

Figure 4a illustrates the predictive accuracy of four kinetic mechanisms (Yan, Wang, Aramco 2.0, and Reuter) for the LBV of methanol at 298 K, clearly showing their agreement with the experimental data from Saeed and Wang under different pressures. The results indicate that under atmospheric pressure, all mechanisms overpredict the LBV under fuel-rich conditions when compared to the experimental data. The mean relative errors for the Yan, Wang, Aramco 2.0, and Reuter mechanisms are 3.33%, 4.17%, 6.10%, and 3.48%, respectively. In this condition, the Wang, Reuter, and Yan mechanisms all demonstrate relatively high predictive accuracy. A more detailed analysis reveals that the accuracy of each mechanism varies across different equivalence ratios. The Reuter mechanism shows the best prediction within the φ = 1.1–1.4, with a mean relative error of 4.37%. In contrast, the Yan mechanism achieves the best prediction within the equivalence ratio range of 0.7–1.0, with a mean relative error of 1.46%. Under a pressure of 0.5 bar, all four mechanisms exhibit high predictive accuracy in the fuel-lean region. However, their predictions fall below the experimental values near the stoichiometric ratio, while overpredictions are observed under fuel-rich conditions. The mean relative errors for the Yan, Wang, Aramco 2.0, and Reuter mechanisms at 0.5 bar are 6.83%, 5.08%, 6.3%, and 5.79%, respectively. Here, the Wang mechanism shows the highest accuracy, while the prediction errors of the other mechanisms are relatively close, making them viable alternatives for application. At a higher pressure of 3 bar, the overall prediction trends of all mechanisms for equivalence ratios below 1.2 are similar to those observed at 0.5 bar. However, in the fuel-rich region, the Wang and Aramco 2.0 mechanisms perform better, with their predictions largely consistent with the experimental data. The mean relative errors at 3 bar are 8.57%, 4.64%, 7.39%, and 8.96% for the Yan, Wang, Aramco 2.0, and Reuter mechanisms, respectively. The Wang mechanism maintains the highest predictive accuracy, although the differences compared to the other mechanisms remain relatively small. The prediction errors of all mechanisms are within 10%. In summary, for predicting methanol's LBV under different pressures, the discrepancies in predictive deviation among all the mechanisms are not substantial. A further analysis will be provided in the following section.

To further investigate the reasons for the discrepancies among different mechanisms, a sensitivity analysis of pure methanol was conducted under atmospheric pressure using various mechanisms to illustrate the differences between the mechanisms. Since the Yan mechanism provides the most accurate predictions under lean conditions, and the Reuter mechanism performs well under rich conditions. Under lean conditions, as shown in Fig. 5a and b, the

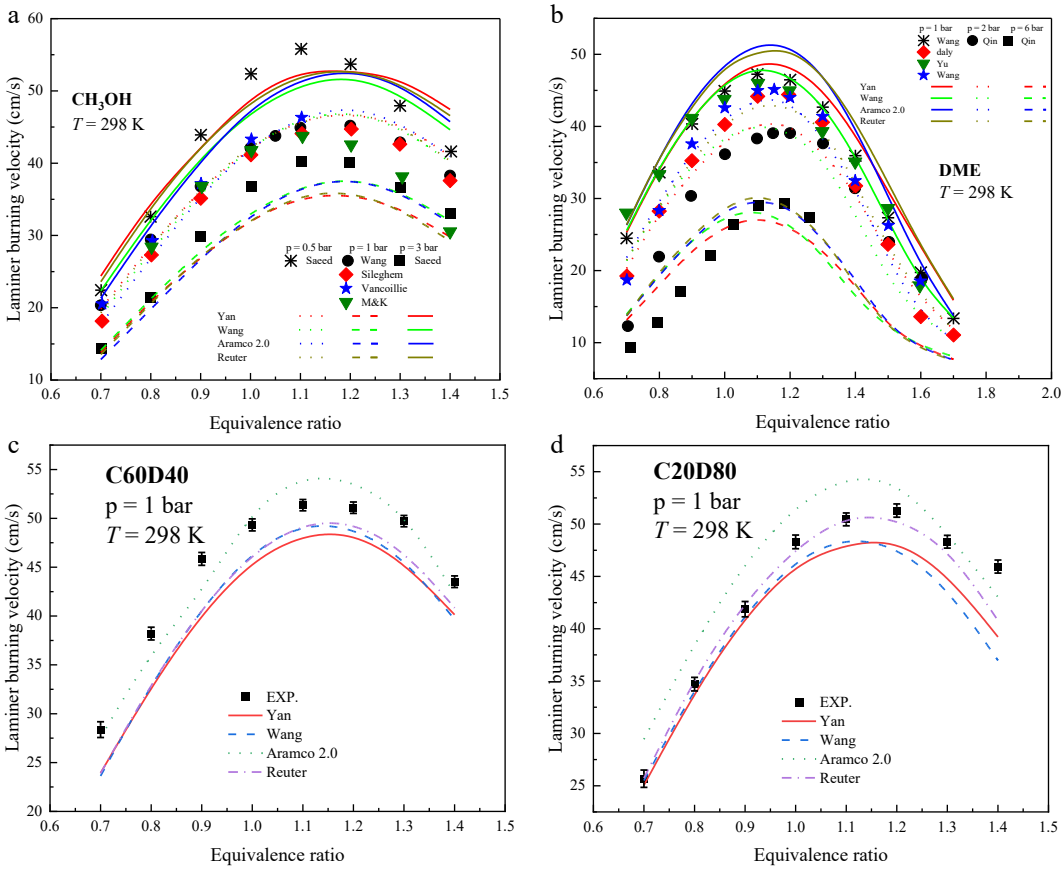

Fig. 4 Variation of LBV of methanol and DME with equivalence ratio: Experimental data (symbols) vs simulation results from various models (lines).

reactions H + O_2 (+M) = HO_2 (+M) and H + O_2 = O + OH have the greatest influence on the LBV in both mechanisms, with their promoting and inhibiting effects being largely consistent. Further analysis shows that the reaction CO + OH = CO_2 + H ranks second in promoting effects in both mechanisms. Under rich conditions, as shown in Fig. 5c and d, reaction H + O_2 = O + OH exhibits the strongest inhibiting effect on flame speed in the Yan mechanism but has the strongest promoting effect in the Reuter mechanism. Conversely, the reaction HCO + H = CO + H_2 has the most significant promoting effect in the Yan mechanism but shows the most significant inhibiting effect in the Reuter mechanism. These differences observed in the sensitivity analyses may explain the discrepancies between the two mechanisms in predicting LBV.

Figure 4b illustrates the predictive accuracy of four kinetic mechanisms (Yan, Wang, Aramco 2.0, and Reuter) for the LBV of DME at 298 K, clearly demonstrating their agreement with the experimental data from Qin and Wang under different pressures. Under atmospheric pressure, the Wang mechanism's prediction curve shows excellent agreement with the experimental data. The mean relative errors for the Yan, Wang, Aramco 2.0, and Reuter mechanisms are 7.58%, 2.36%, 8.18%, and 11.37%, respectively. A more detailed analysis reveals that the accuracy of each mechanism varies across different equivalence ratios. In the fuel-lean region (equivalence ratio 0.7–1.0), the Yan and Wang mechanisms demonstrate the highest predictive accuracy, with mean relative errors of 2.71% and 3.05%, respectively. In the fuel-rich region (equivalence ratio 1.1–1.7), the Wang mechanism achieves the best accuracy with a mean relative error of 0.53%. At 2 bar, the mean relative errors for the Yan, Wang, Aramco 2.0, and Reuter mechanisms are 14.53%, 20.12%, 21.4%, and 18.32%, respectively. The Aramco 2.0 and Reuter mechanisms show higher accuracy in the fuel-rich region, while the Yan and Wang mechanisms perform better near the stoichiometric ratio. However, in the fuel-lean region, all mechanisms deviate from the experimental data, with overall over-predictions. At 6 bar, the mean relative errors are 19.82%, 25.62%, 24.83%, and 23.44% for the Yan, Wang, Aramco 2.0, and Reuter mechanisms, respectively. The Aramco 2.0 and Reuter mechanisms exhibit relatively high accuracy in the slightly fuel-rich region, followed by the Yan and Wang mechanisms. The predictions in the fuel-lean region are consistent with the trends observed at 2 bar. In summary, under high-pressure conditions, the Yan mechanism should be prioritized due to its highest predictive accuracy. Under atmospheric pressure, the Wang mechanism is the preferred choice, followed by the Aramco 2.0 and Yan mechanisms.

To further investigate the reasons for the differences among mechanisms, a sensitivity analysis was conducted for the Yan and Wang mechanisms under lean and rich conditions for pure DME combustion. Under lean conditions, as shown in Fig. 6a and b, the reaction H + O_2 = O + OH exhibits the strongest promoting effect on flame speed in the Wang mechanism, but it plays the most inhibiting role in the Yan mechanism. In contrast, in the Yan mechanism, the reaction H + O_2 (+M) = HO_2 (+M) shows the strongest promoting effect, while in the Wang mechanism this reaction ranks second among the most inhibiting reactions. However, both mechanisms predict nearly identical flame speeds under these lean conditions, suggesting that these reaction-level differences have little overall impact on flame speed in this regime. Under rich conditions, as shown in Fig. 6c and d, both mechanisms identify the H + O_2 = O + OH reaction as the most inhibiting for LBV. However, there are significant differences in the key promoting reactions. In the Wang

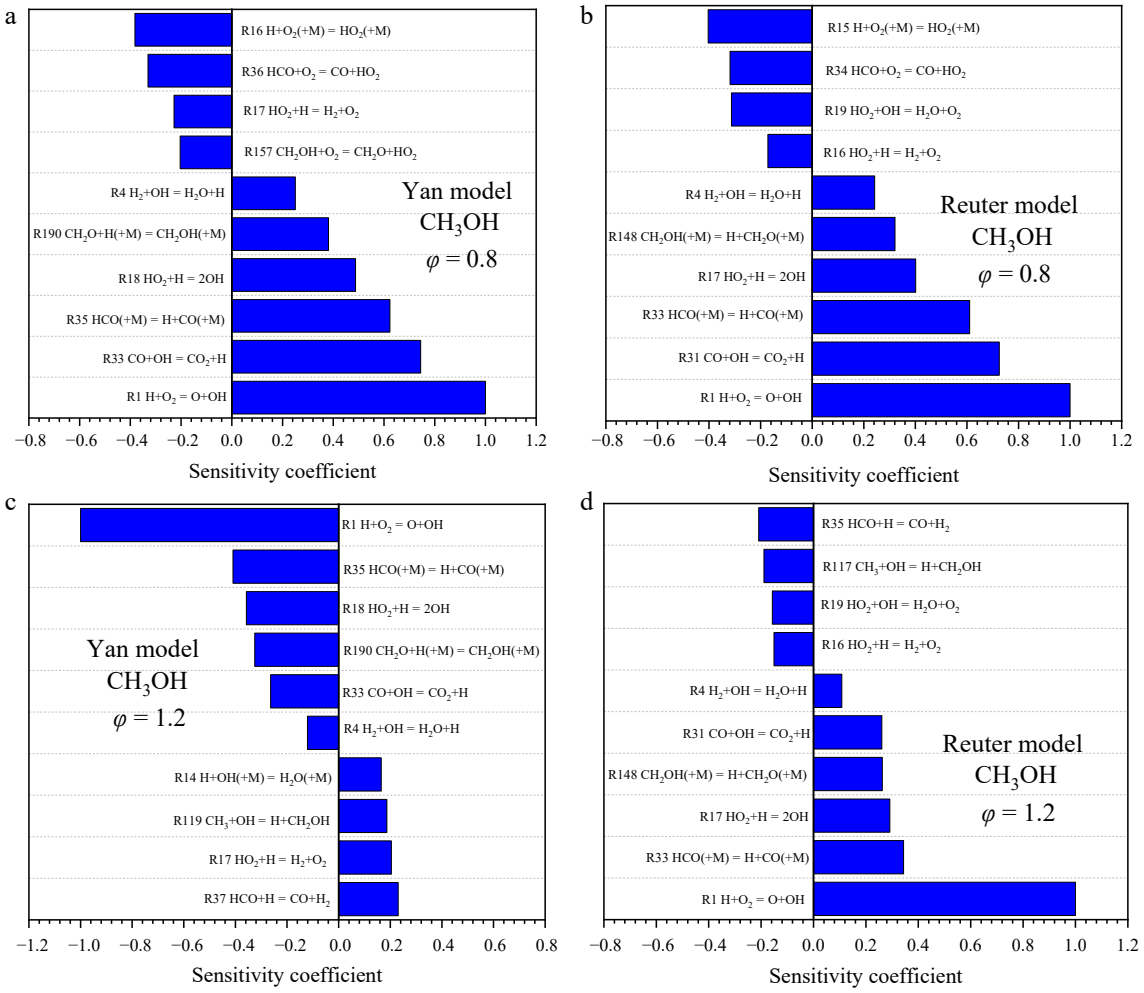

Fig. 5 Sensitivity analysis of the Yan and Reuter models at different equivalence ratios.

mechanism, the reaction H + OH + M = H_2O + M provides the greatest promoting effect, whereas in the Yan mechanism, the most significant promoting reaction is HCO + H = CO + H_2. The CO and H_2 produced in the Yan mechanism may explain why it predicts a higher LBV than the Wang mechanism at φ = 1.2.

In Fig. 4c, the LBV of the C60D40 mixture was calculated with detailed mechanisms. Results show that the average relative errors compared with experimental data are 9.54%, 4.42%, 8.01%, and 8.79% for the Yan, Aramco 2.0, Reuter, and Wang mechanisms, respectively. It can be observed that the primary error of the Aramco 2.0 mechanism at this point arises primarily from rich operating conditions in φ = 1.0–1.3, indicating significant room for improvement in the mechanism's performance under these specific conditions. In Fig. 4d, the LBV of the C20D80 mixture was simulated. The results indicate that the Reuter mechanism delivers the best prediction for the mixture, with an average relative error of 2.43%, whilst the Yan, Wang, and Aramco 2.0 mechanisms show average relative errors of 5.18%, 5.58%, and 8.26% respectively. It can be observed that the Reuter mechanism exhibits a significant deviation at an equivalence ratio of 1.4, indicating a particular opportunity for improvement in its performance under this specific condition.

To further illustrate the predictive differences among mechanisms at various blend ratios, sensitivity analysis was conducted using C20D80 as an example. For both lean and rich conditions, the Reuter mechanism, known for its high prediction accuracy across blend ratios, was selected for analysis. Additionally, the Aramco 2.0 mechanism, which performs best at 60% DME, was also analyzed. Under lean conditions (Fig. 7a, b), the sensitivity analysis revealed that the reactions O_2 + H = O + OH and H + O_2 (+M) = HO_2 (+M) are the most influential on LBV in both mechanisms, acting as the strongest inhibitor and promoter, respectively. A difference in the second most significant promoting elementary reaction is likely the cause of the higher predictions made by the Aramco 2.0 mechanism. Under rich conditions (Fig. 7c, d), the elementary reactions significantly affecting LBV show considerable consistency between the two mechanisms. However, there exists a notable discrepancy in their predicted LBV. This disparity is primarily attributed to differences in the sensitivity coefficients of the same key reactions within each mechanism.

In summary, the Yan mechanism is recommended as the priority choice under high-pressure conditions, as it demonstrates satisfactory performance for both pure methanol and pure DME. Under atmospheric pressure, the Aramco 2.0 mechanism is primarily recommended due to its good performance for methanol, DME, and methanol/DME blended fuels.

Species concentration analysis

Methanol and DME are both low-carbon, oxygenated fuels. When blended and used in engines, in addition to producing conventional emissions such as CO and CO_2, they also generate unconventional emissions like CH_2O. In light of this, to more comprehensively

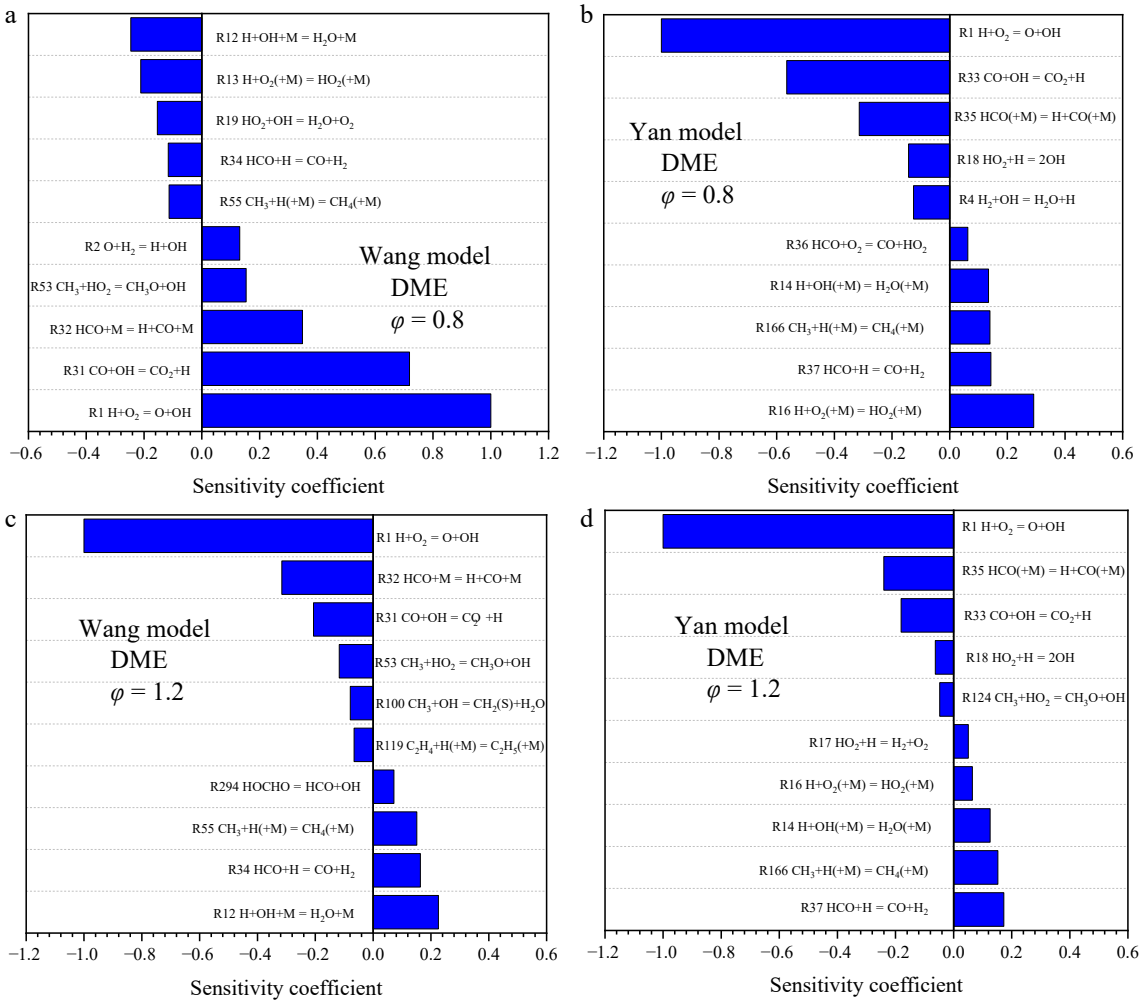

Fig. 6 Sensitivity analysis of the Wang and Yan models at different equivalence ratios.

evaluate the performance of different chemical kinetic mechanisms, species concentration validations were further conducted for the Yan, Wang, Aramco 2.0, and Reuter mechanisms using experimental data from jet stirred reactor studies by Burke et al. and Yan et al.[19,44] (as summarized in Table 2).

Figure 8a shows the temperature-dependent concentrations of CO, CO_2, and CH_2O during methanol oxidation in the JSR. It is evident that all four mechanisms can predict the experimental data with reasonable accuracy, with deviations falling within experimental uncertainty. However, the Aramco 2.0 mechanism results align more closely with the experimental values. Figure 8b displays the temperature-dependent concentrations of CO, CO_2, and CH_2O during DME oxidation in the JSR. It can be clearly observed that all four mechanisms overestimate CH_2O concentrations at 800 K, but under most conditions they can predict the experimental data accurately. Moreover, the Yan mechanism predictions generally match the experimental data better across most conditions. This is understandable, as the Yan mechanism was specifically developed based on this experimental data. Overall, both the Aramco 2.0 and Yan mechanisms produce satisfactory predictions.

To clarify the cause of the prediction deviations at 800 K, Fig. 9 presents the CH_2O sensitivity analyses at 800 K using the Yan and Wang mechanisms. The analysis shows that for two mechanisms, the reaction $CH_3OCH_3 + OH = CH_3OCH_2 + H_2O$ is the most significant promoting reaction. However, their most dominant inhibiting reactions differ. For the Yan mechanism, $CH_3OCH_2 = CH_3 + CH_2O$ is the most inhibiting reaction, while for the Wang mechanism, $CH_2OCH_2O_2H = OH + 2CH_2O$ plays this role. This difference accounts for the discrepancy in their CH_2O predictions. Figure 10 shows the CH_2O formation pathways for DME at 800 K with a conversion of 20% using the Yan and Wang mechanisms. It can be observed that in both the Yan and Wang mechanisms, the primary pathway for CH_2O formation is $CH_3OCH_3 \rightarrow CH_3OCH_2 \rightarrow CH_3OCH_2O_2 \rightarrow CH_2OCH_2O_2H \rightarrow CH_2O$. The formed CH_2O subsequently reacts with radicals such as OH and HO_2 to produce CO and H_2O. Compared to the Wang mechanism, the Yan mechanism includes an additional consumption pathway for CH_2O: $CH_2O \rightarrow H_2O_2 \rightarrow H_2O$. The underestimation of CH_2O concentration at 800 K is likely attributed to two main reasons: first, the rate constants in the reaction pathways responsible for CH_2O formation may be underestimated, leading to lower CH_2O concentrations; second, the rate constants in the consumption pathways may be overestimated, which would also result in reduced CH_2O levels. In subsequent reaction kinetics studies, the relevant rate constants should be adjusted to improve the predictive accuracy of the mechanism.

The Yan mechanism was employed to simulate pure methanol, C60D40, and C20D80 blends under conditions identical to Burke et al.[44] (Fig. 8c), in order to investigate the temperature-dependent concentration trends of CO, CO_2, and CH_2O between 700 and 1,200 K for different mixing ratios. A key finding is that the

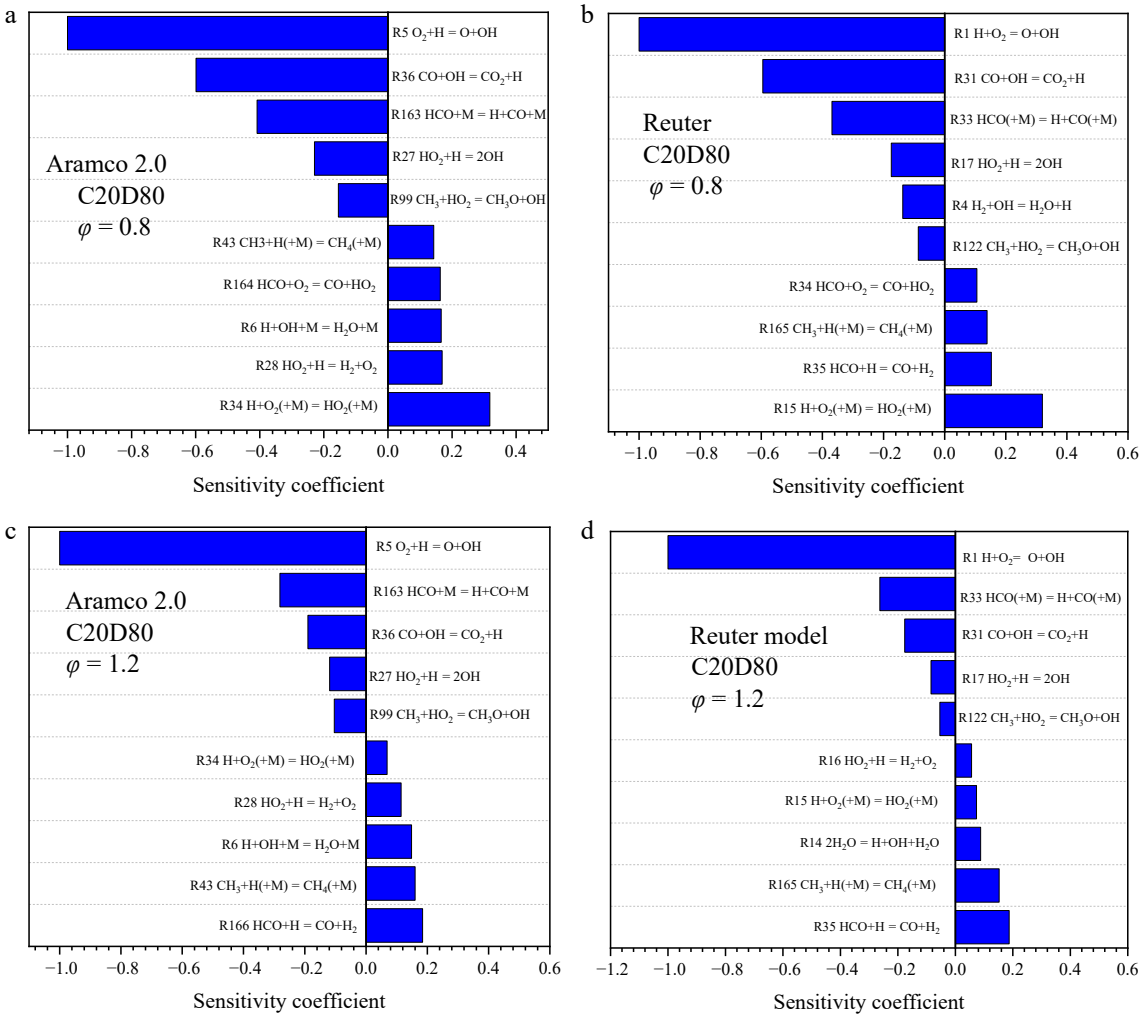

Fig. 7 Sensitivity analysis of the Aramco 2.0 and Reuter models at different equivalence ratios.

evolution of the concentrations of CH_2O and CO first increase, and then decrease with rising temperature, while CO_2 concentration shows a continuously increasing trend. The concentration variations of these three species do not follow a simple linear trend with increasing DME content. For example, CO concentration first increases and then decreases as the DME proportion rises.

Conclusions

The accurate description of the combustion process of methanol/DME is important for fundamental and application combustion studies. However, a comprehensive and comparative assessment of recently developed combustion kinetic mechanisms for these fuels is notably absent. This study employed kinetic simulations to assess six up-to-date reaction mechanisms against a comprehensive dataset, which included ignition delay times (IDT), laminar burning velocities (LBV) of methanol/DME, and key species concentrations during oxidation. The following conclusions were drawn.

Simulation of the IDT for methanol/DME mixtures showed that the Yan, Wang, Reuter, and Aramco 2.0 mechanisms can accurately predict the IDT, with the Yan mechanism exhibiting the highest accuracy. Sensitivity analysis revealed significant differences in the most sensitive inhibiting reactions between the Yan mechanism and the Aramco 2.0 mechanism. When the DME mole fraction reaches 75%, the most dominant promoting and inhibiting reactions differ significantly from those at 25% and 50%.

In terms of LBV, under high-pressure conditions, the Yan mechanism demonstrates satisfactory predictive performance for both methanol and DME. At atmospheric pressure, the Aramco 2.0 mechanism is recommended as the preferred choice, as it performs well for methanol, DME, and methanol/DME blended fuels. Sensitivity analysis conducted with different mechanisms reveals that the varying sensitivities of elementary steps under identical conditions are identified as the fundamental cause of the predictive discrepancies among the mechanisms.

In terms of predicting the concentrations of major intermediate species, the Aramco 2.0 and Yan mechanisms exhibited overall smaller prediction deviations and were able to accurately reproduce the temperature-dependent variation trends of CO, CO_2, and CH_2O. Sensitivity analysis and reaction pathway analysis revealed that differences in key promoting and inhibiting reactions, as well as radical consumption pathways are the main reasons for the discrepancies in predictions among different mechanisms. Simulations of methanol/DME mixtures with varying blending ratios using the Yan mechanism showed that the concentration changes of different species do not follow a simple linear trend with increasing DME content.

Therefore, for future practical industrial applications of methanol/DME blended fuels, both the Yan and Aramco 2.0 mechanisms are

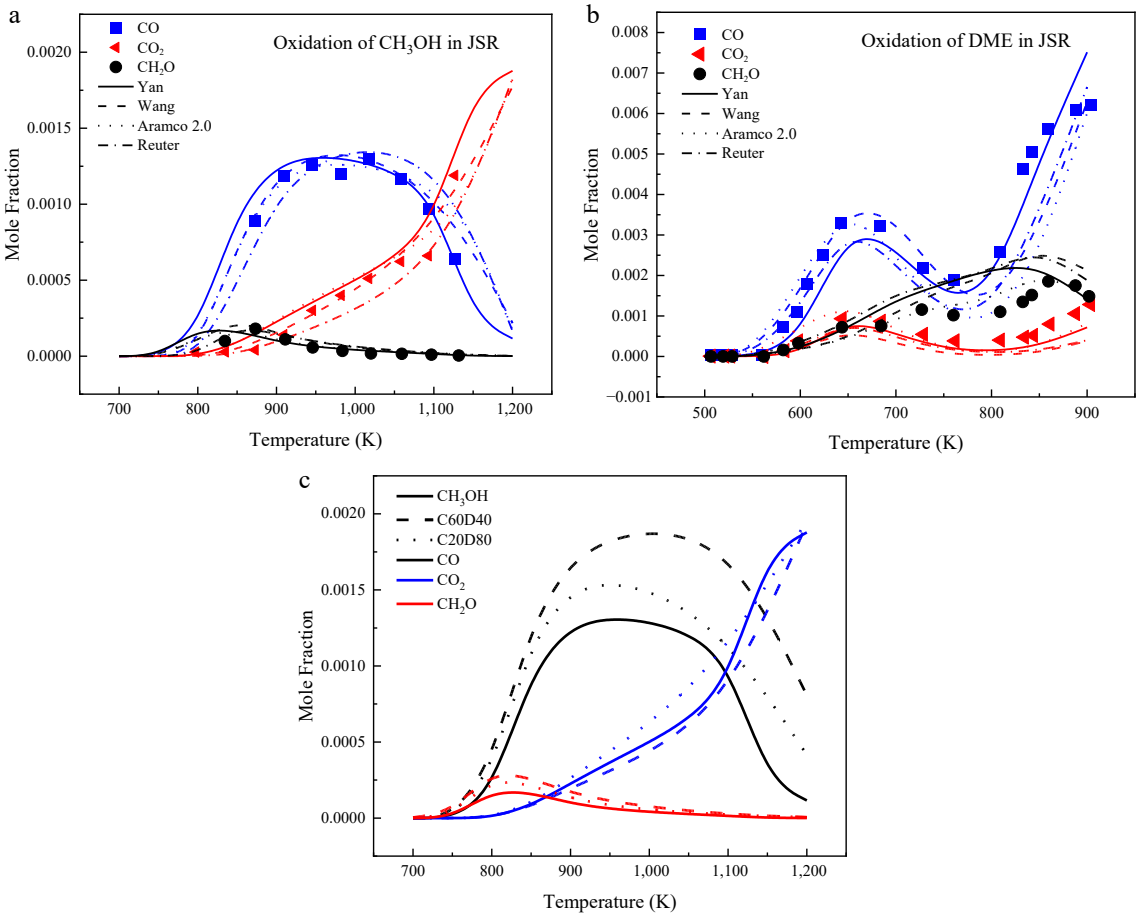

Fig. 8 Key species analysis for methanol/DME oxidation. (a), (b) Temperature dependence of species concentrations: Experimental data (symbols) vs simulation results from various models (lines). (c) Variations in species concentration with temperature under different blending ratios with the Yan mechanism.

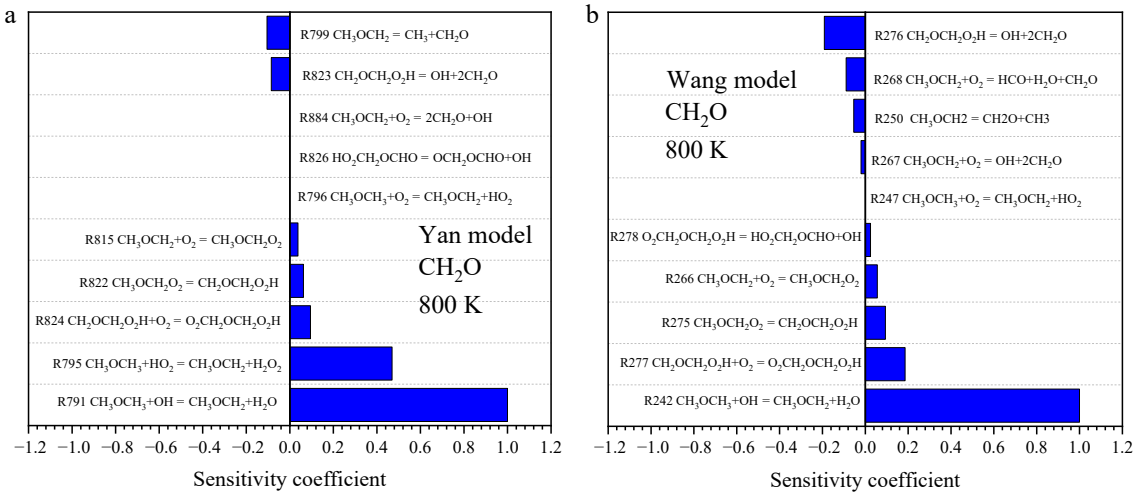

Fig. 9 Sensitivity analysis of different models. (a) Sensitivity analysis of CH_2O by Yan model, (b) sensitivity analysis of CH_2O by Wang model.

promising, as they can provide acceptable predictions for IDT, LBV, and species concentrations. The Yan mechanism exhibits superior performance under high-pressure conditions, whereas the Aramco 2.0 mechanism is relatively more suitable for use at atmospheric pressure. They have the potential for broader application in future engine combustion studies and simulations. In future work, it is still necessary to further supplement experimental data on the laminar combustion and low-temperature oxidation behavior of methanol/DME blends, and to continuously optimize kinetic mechanisms based on experimental results to gain deeper insights into their applicability in real engines.

Author contributions

The authors confirm contribution to the paper as follows: writing – review and editing, conceptualization, funding acquisition, formal

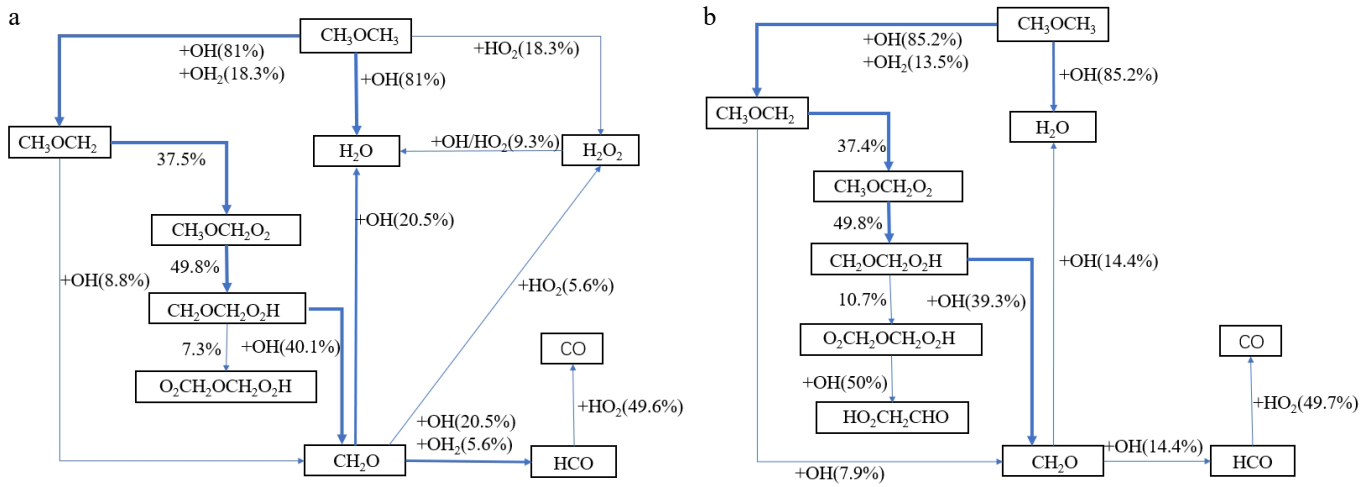

Fig. 10 Reaction pathway analysis of different models. (a) Reaction path analysis of Yan model, (b) reaction path analysis of Wang model.

analysis, supervision, project administration: Xiao H; writing – original draft, conceptualization, methodology, investigation, data curation: Xie C; writing – original draft, investigation, formal analysis, visualization: Ma Z; writing – review and editing, resources, supervision: Liang Y; methodology, formal analysis, supervision: Li X. All authors reviewed the result and approved the final version of the manuscript.

Data availability

The datasets generated during and/or analyzed in the current study are available from the corresponding author on reasonable request.

Acknowledgments

This work was supported by Guangzhou Education Bureau's 2024 University Research Project (No. 2024312533), 2023 Basic and Applied Basic Research Project of Guangzhou Municipal Bureau of Science and Technology (No. SL2022A04J00794).

Conflict of interest

The authors declare that they have no conflict of interest.

Dates

Received 22 August 2025; Revised 30 December 2025; Accepted 22 January 2026; Published online 14 May 2026

References

[1] Shih CF, Zhang T, Li J, Bai C. 2018. Powering the future with liquid sunshine. *Joule* 2(10):1925–1949

[2] Li J, Zhu X, Djilali N, Yang Y, Ye D, et al. 2022. Comparative well-to-pump assessment of fueling pathways for zero-carbon transportation in China: hydrogen economy or methanol economy? *Renewable and Sustainable Energy Reviews* 169:112935

[3] Eggemann L, Escobar N, Peters R, Burauel P, Stolten D. 2020. Life cycle assessment of a small-scale methanol production system: a Power-to-Fuel strategy for biogas plants. *Journal of Cleaner Production* 271:122476

[4] Harris K, Grim RG, Huang Z, Tao L. 2021. A comparative techno-economic analysis of renewable methanol synthesis from biomass and CO_2: opportunities and barriers to commercialization. *Applied Energy* 303:117637

[5] Li Y, Jia M, Chang Y, Liu Y, Xie M, et al. 2014. Parametric study and optimization of a RCCI (reactivity controlled compression ignition) engine fueled with methanol and diesel. *Energy* 65:319–332

[6] Yin X, Yue G, Liu J, Duan H, Duan Q, et al. 2023. Investigation into the operating range of a dual-direct injection engine fueled with methanol and diesel. *Energy* 267:126625

[7] Chen X, Wang H, Song C, Wang W, Huang J, et al. 2014. Investigation of the cold-start engine performance at a low temperature for an engine fuelled with alternative fuel. *Proceedings of the Institution of Mechanical Engineers, Part D: Journal of Automobile Engineering* 228(3):310–318

[8] Liu H, Zhang X, Zhang Z, Wu Y, Wang C, et al. 2023. Effects of 2-ethylhexyl nitrate (EHN) on combustion and emissions on a compression ignition engine fueling high-pressure direct-injection pure methanol fuel. *Fuel* 341:127684

[9] Cheng C, Faurskov Cordtz R, Berg Thomsen T, Langballe Førby N, Schramm J. 2022. Application of methanol with an ignition improver in a small marine CI engine. *Energy Conversion and Management* 271:116311

[10] Sezer İ. 2020. A review study on using diethyl ether in diesel engines: effects on fuel properties, injection, and combustion characteristics. *Energy & Environment* 31(2):179–214

[11] Xu Z, Wang J, Zhao P, Jia M, Chang Y, et al. 2024. Exploring energy utilization of the methanol/dimethyl ether dual-fuel engine under the methanol reforming strategy: a comparison of different low-temperature combustion modes. *Energy* 312:133659

[12] Calam A, Aydoğan B, Halis S. 2020. The comparison of combustion, engine performance and emission characteristics of ethanol, methanol, fusel oil, butanol, isopropanol and naphtha with n-heptane blends on HCCI engine. *Fuel* 266:117071

[13] Jang J, Yang K, Bae C. 2009. The effect of injection location of DME and LPG in a dual fuel HCCI engine. *Powertrains, Fuels and Lubricants Meeting, Florence, Italy, June 15, 2009*. SAE International. doi: 10.4271/2009-01-1847

[14] Yao M, Huang C, Zheng Z. 2007. Multidimensional numerical simulation on dimethyl ether/methanol dual-fuel homogeneous charge compression ignition (HCCI) engine combustion and emission processes. *Energy & Fuels* 21(2):812–821

[15] Lee H, Lim O. 2016. A computational study of DME-methanol fractions with controlling several factors on HCCI combustion. *Journal of Mechanical Science and Technology* 30(4):1931–1941

[16] Taghavifar H, Nemati A, Walther JH. 2019. Combustion and exergy analysis of multi-component diesel-DME-methanol blends in HCCI engine. *Energy* 187:115951

[17] Wang H, Fang R, Weber BW, Sung CJ. 2018. An experimental and modeling study of dimethyl ether/methanol blends autoignition at low temperature. *Combustion and Flame* 198:89–99

[18] Song W, Tingas EA, Im HG. 2018. A computational analysis of methanol autoignition enhancement by dimethyl ether addition in a counterflow mixing layer. *Combustion and Flame* 195:84–98
[19] Yan C, Zhao H, Wang Z, Song G, Lin Y, et al. 2022. Low-and intermediate-temperature oxidation of dimethyl ether up to 100 atm in a supercritical pressure jet-stirred reactor. *Combustion and Flame* 243:112059
[20] Burke U, Somers KP, O'Toole P, Zinner CM, Marquet N, et al. 2015. An ignition delay and kinetic modeling study of methane, dimethyl ether, and their mixtures at high pressures. *Combustion and Flame* 162(2):315–330
[21] Wang Z, Zhang X, Xing L, Zhang L, Herrmann F, et al. 2015. Experimental and kinetic modeling study of the low-and intermediate-temperature oxidation of dimethyl ether. *Combustion and Flame* 162(4):1113–1125
[22] Hashemi H, Christensen JM, Glarborg P. 2019. High-pressure pyrolysis and oxidation of DME and DME/CH_4. *Combustion and Flame* 205:80–92
[23] Reuter CB, Zhang R, Yehia OR, Rezgui Y, Ju Y. 2018. Counterflow flame experiments and chemical kinetic modeling of dimethyl ether/methane mixtures. *Combustion and Flame* 196:1–10
[24] Pelucchi M, Cavallotti C, Faravelli T, Klippenstein SJ. 2018. H-Abstraction reactions by OH, HO_2, O, O_2 and benzyl radical addition to O_2 and their implications for kinetic modelling of toluene oxidation. *Physical Chemistry Chemical Physics* 20(16):10607–10627
[25] Klippenstein SJ. 2017. From theoretical reaction dynamics to chemical modeling of combustion. *Proceedings of the Combustion Institute* 36(1):77–111
[26] Klippenstein SJ, Sivaramakrishnan R, Burke U, Somers KP, Curran HJ, et al. 2022. $H\dot{O}_2$+ $H\dot{O}_2$: high level theory and the role of singlet channels. *Combustion and Flame* 243:111975
[27] Zhao H, Yan C, Song G, Wang Z, Jasper AW, et al. 2024. High-pressure oxidation of hydrogen diluted in N_2 with added H_2O or CO_2 at 100 atm in a supercritical-pressure jet-stirred reactor. *Combustion and Flame* 266:113543
[28] Mulvihill CR, Danilack AD, Goldsmith CF, Demireva M, Sheps L, et al. 2021. Non-Boltzmann effects in chain branching and pathway branching for diethyl ether oxidation. *Energy & Fuels* 35(21):17890–17908
[29] Zhao H, Yang X, Ju Y. 2016. Princeton HP-Mech. Kinetic studies of ozone assisted low temperature oxidation of dimethyl ether in a flow reactor using molecular-beam mass spectrometry. *Combustion and Flame* 173:187–194
[30] Carr SA, Still TJ, Blitz MA, Eskola AJ, Seakins PW, et al. 2013. Experimental and theoretical study of the kinetics and mechanism of the reaction of OH radicals with dimethyl ether. *The Journal of Physical Chemistry A* 117(44):11142–11154
[31] Sivaramakrishnan R, Michael JV, Wagner AF, Dawes R, Jasper AW, et al. 2011. Roaming radicals in the thermal decomposition of dimethyl ether: experiment and theory. *Combustion and Flame* 158(4):618–632
[32] Marshall P, Glarborg P. 2015. Ab initio and kinetic modeling studies of formic acid oxidation. *Proceedings of the Combustion Institute* 35(1):153–160
[33] De Goey LPH, Somers LMT, Bosch WMML, Mallens RMM. 1995. Modeling of the small scale structure of flat burner-stabilized flames. *Combustion Science and Technology* 104(4–6):387–400
[34] Wang Z, Han X, He Y, Zhu R, Zhu Y, et al. 2021. Experimental and kinetic study on the laminar burning velocities of NH_3 mixing with CH_3OH and C_2H_5OH in premixed flames. *Combustion and Flame* 229:111392
[35] Saeed K, Stone CR. 2004. Measurements of the laminar burning velocity for mixtures of methanol and air from a constant-volume vessel using a multizone model. *Combustion and Flame* 139(1–2):152–166
[36] Sileghem L, Alekseev VA, Vancoillie J, Nilsson EJK, Verhelst S, et al. 2014. Laminar burning velocities of primary reference fuels and simple alcohols. *Fuel* 115:32–40
[37] Vancoillie J, Christensen M, Nilsson EJK, Verhelst S, Konnov AA. 2012. Temperature dependence of the laminar burning velocity of methanol flames. *Energy & Fuels* 26(3):1557–1564
[38] Metghalchi M, Keck JC. 1982. Burning velocities of mixtures of air with methanol, isooctane, and indolene at high pressure and temperature. *Combustion and Flame* 48:191–210
[39] Wang Z, Wang S, Whiddon R, Han X, He Y, et al. 2018. Effect of hydrogen addition on laminar burning velocity of CH_4/DME mixtures by heat flux method and kinetic modeling. *Fuel* 232:729–742
[40] Qin X, Ju Y. 2005. Measurements of burning velocities of dimethyl ether and air premixed flames at elevated pressures. *Proceedings of the Combustion Institute* 30(1):233–240
[41] Yu H, Hu E, Cheng Y, Yang K, Zhang X, et al. 2015. Effects of hydrogen addition on the laminar flame speed and markstein length of premixed dimethyl ether–air flames. *Energy & Fuels* 29(7):4567–4575
[42] Daly CA, Simmie JM, Würmel J, Djebaïli N, Paillard C. 2001. Burning velocities of dimethyl ether and air. *Combustion and Flame* 125(4):1329–1340
[43] Wang YL, Holley AT, Ji C, Egolfopoulos FN, Tsotsis TT, et al. 2009. Propagation and extinction of premixed dimethyl-ether/air flames. *Proceedings of the Combustion Institute* 32(1):1035–1042
[44] Burke U, Metcalfe WK, Burke SM, Heufer KA, Dagaut P, et al. 2016. A detailed chemical kinetic modeling, ignition delay time and jet-stirred reactor study of methanol oxidation. *Combustion and Flame* 165:125–136
[45] Xiao H, Valera-Medina A, Bowen PJ. 2017. Study on premixed combustion characteristics of co-firing ammonia/methane fuels. *Energy* 140:125–135
[46] Chu X, Li X, Gao P, Ma Z, Xiao H, et al. 2024. High-temperature autoignition characteristics of NH_3-H_2-CH_4. *Fuel* 365:131228
[47] Olm C, Zsély IG, Pálvölgyi R, Varga T, Nagy T, et al. 2014. Comparison of the performance of several recent hydrogen combustion mechanisms. *Combustion and Flame* 161(9):2219–2234